Published in final edited form as:
Biomaterials. 2011 September ; 32(25): 5906–5914. doi:10.1016/j.biomaterials.2011.04.069.

Encapsulation of Curcumin in Self-Assembling Peptide Hydrogels as Injectable Drug Delivery Vehicles

Aysegul Altunbas
Department of Materials Science and Engineering and Delaware Biotechnology Institute 201 DuPont Hall, University of Delaware Newark, DE 19716 (USA)

Seung Joon Lee[Dr.] and **Sigrid A. Rajasekaran[Asst. Prof.]**
Cancer Epigenetics Laboratory Nemours Center for Childhood Cancer Research A.I. duPont Hospital for Children Wilmington, DE 19803

Joel P. Schneider[Prof.]
Chemical Biology Laboratory Center for Cancer Research, National Cancer Institute Frederick, MD 21702

Darrin J. Pochan*[Prof.]
Department of Materials Science and Engineering and Delaware Biotechnology Institute 201 DuPont Hall, University of Delaware Newark, DE 19716 (USA)

Abstract

Curcumin, a hydrophobic polyphenol, is an extract of turmeric root with antioxidant, anti-inflammatory and anti-tumorigenic properties. Its lack of water solubility and relatively low bioavailability set major limitations for its therapeutic use. In this study, a self-assembling peptide hydrogel is demonstrated to be an effective vehicle for the localized delivery of curcumin over sustained periods of time. The curcumin-hydrogel is prepared *in-situ* where curcumin encapsulation within the hydrogel network is accomplished concurrently with peptide self-assembly. Physical and *in vitro* biological studies were used to demonstrate the effectiveness of curcumin-loaded β-hairpin hydrogels as injectable agents for localized curcumin delivery. Notably, rheological characterization of the curcumin loaded hydrogel before and after shear flow have indicated solid-like properties even at high curcumin payloads. *In vitro* experiments with a medulloblastoma cell line confirm that the encapsulation of the curcumin within the hydrogel does not have an adverse effect on its bioactivity. Most importantly, the rate of curcumin release and its consequent therapeutic efficacy can be conveniently modulated as a function of the concentration of the MAX8 peptide.

Keywords

Peptide; Self-assembly; Curcumin; Hydrogel

1. Introduction

The need for biocompatible, high water content materials that facilitate the transport of metabolites was emphasized by Wichterle and Lim in 1960 [1] who highlighted likely structural and biological incompatibility between conventional plastics and living tissue. Preparation of the first synthetic hydrogel by these scientists marked the beginning of a new

* pochan@udel.edu .

era in modern hydrogel research. Since then hydrogels - highly hydrated, porous materials produced through chemical and/or physical crosslinking of molecules - have received remarkable scientific interest in the field of biomedical research [2–5]. The ability to conveniently tune the physical and chemical properties of hydrogels through changes in the constituent molecule chemical functionality, architecture as well as microenvironment (solution conditions etc.) have led to their application in fields such as tissue engineering, drug delivery and medical implants [3,5,6].

For delivery applications, hydrogels have been used to incorporate drug molecules into the gel matrix to create reservoirs that deliver bioactive agents [7]. Some of the key issues that drug delivery studies try to address include increasing bioavailability of drugs, reducing side effects, controlling kinetic release profiles, increasing clinical ease of use and reducing pain from administration. Localized drug delivery is especially desirable to increase the efficacy of highly metabolized drugs when administered conventionally, to circumvent natural barriers such as the blood-brain barrier and to reduce serious side effects of systemically administered toxic drugs. The necessity to deliver drugs for the efficacious treatment of diseases has resulted in significant advances in the development of injectable drug delivery vehicles [8,9].

Currently, hydrogels are primarily designed to exist as free flowing polymer solutions *ex vivo* to enable injection as a low viscosity liquid and subsequently gel *in vivo* through crosslinking induced by stimuli such as radiation, enzymes, salt or temperature [10–12]. Although there are a number of advantages associated with injectable liquids that can be crosslinked into hydrogels after injection, the most important being that they facilitate local delivery of drug molecules, there are also significant limitations. Some of these limitations are toxicity of un-reacted monomers, a high degree of crystallinity in pre-crosslinked synthetic polymers, shrinkage or brittleness of the polymer gels post-crosslinking, and a large amount of drug discharge during the initial burst release in drug delivery vehicles [8]. In addition, ultraviolet radiation used during many *in situ* network formation strategies, or high local temperatures caused by covalent crosslinking chemical reactions, can be detrimental to cells or drug payloads mixed with the network-forming molecules. Finally, even with successful *in vivo* hydrogel formation, the final material and *in vivo* area are affected unavoidably by dilution from bodily fluids, before and during crosslinking, and flow into neighboring tissues prior to significant crosslinking, respectively. In this context, nano-engineered delivery systems can provide innovative solutions to overcome the limitations of conventional injectable liquid, polymer-based systems [13].

Self-assembling systems in which water soluble peptides undergo sol-gel transition in response to changes in ionic strength [14], temperature [15, 6], or pH [17–23] of the medium represent an area of growing interdisciplinary research. Mixing induced, two-component physical hydrogels and enzyme catalyzed self-assembly have also been reported [24–27]. Gelation in such systems is achieved through non-covalent, physical crosslinking by secondary forces such as hydrophobic and Van der Waals interactions, as well as ionic and hydrogen bonding [28]. Biocompatibility, hydrophilicity and physiologically benign processing conditions are some of the beneficial properties that make physically crosslinked peptide hydrogels attractive candidates as injectable delivery vehicles for therapeutic agents [28]. Importantly, the ability to modulate the bulk physical behavior, such as network stiffness and porosity, of the hydrogel by changing its local nanostructure or network architecture is a potent feature of peptide-based hydrogels. Such changes may be introduced by changing the peptide primary sequence (constituent amino acids) that dictates the assembled nanostructure, network architecture or the assembly kinetics of the hydrogel material [29–31].

We have developed a self-assembling peptide hydrogel system that can form a solid physical hydrogel by *in vitro* assembly at physiological conditions such as provided by cell culture medium. The physical gelation at physiological conditions allows three-dimensional, homogeneous encapsulation of desired molecules and/or cells [30,32]. Moreover, these peptide hydrogels display shear-thinning and immediate recovery properties that make them excellent candidates for injectable therapies. More specifically, a gel formed *ex vivo*; with desired stiffness, porosity, nanostructure, encapsulated payload, etc.; has the ability to flow with low viscosity while under shear and immediately recover back to a solid hydrogel on cessation of shear [14,30,33]. This shear-thinning and immediate recovery enables injection, without syringe-clogging, to a specific site and provides site specificity due to immediate solid-like properties of gel after injection. Also, this design yields hydrogels with the same material properties (stiffness, porosity, nanostructure, payload distribution), both before and after injection [30,33], as opposed to injected liquids where changes in materials properties and volume from observed *in vitro* behavior can occur due to dilution and flow. In addition, the peptide hydrogels do not swell after formation, either before or after injection, when exposed to additional solution or bodily fluids. Rather, new solutes and aqueous fluids can begin to diffuse into and within the stable hydrogels as defined by the porosity of the self-assembled peptide network. A schematic showing the self-assembly pathway of the peptide MAX8 used in this study is displayed in Figure 1(a). MAX8 [30], a 20 amino acid peptide, is composed of two arms of alternating lysine and valine residues surrounding a four residue sequence (-V^{D}PPT-) which is known to adopt a type II` turn under appropriate solution conditions. A single lysine residue is replaced with a glutamic acid residue at the fifteenth position for the overall composition of VKVKVKVKV^{D}PPTKVEVKVKV-NH_2. Due to the charged nature of lysine groups, the peptide adopts an unfolded, random coil structure when dissolved in deionized (DI) water. Self-assembly of peptides can be triggered by changing the ionic strength [14], pH [19] and temperature [15] of the aqueous environment. An increase in ionic strength is obtained by adding cell culture media to the peptide dissolved in water. The salt ions in cell culture media screen the electrostatic repulsions between lysine residues allowing the peptide to fold into a β-hairpin [14, 30]. When folded, MAX8 peptide is stabilized by intrastrand hydrogen bonding and hydrophobic contacts and displays hydrophobic valine and hydrophilic lysine residues on opposite faces of the β-hairpin [34]. Hydrophobic interactions between valine faces of the hairpins cause peptide bilayer formation through hydrophobic collapse. Fibril formation is achieved by intermolecular hydrophobic side chain contacts and lateral hydrogen bonding, along the long axis of the fibril. Figure 1(b) displays a transmission electron microscope (TEM) image of negatively stained MAX8 fibrils. Fibril branching [35] and fibril entanglements account for the mechanical rigidity of the hydrogel.

The polyphenolic compound curcumin (diferuloylmethane) is isolated from the rhizomes of turmeric (*Curcuma longa*), which is a member of the ginger family [36]. The potent therapeutic properties of curcumin for a variety of conditions such as respiratory diseases, liver disorders and diabetic wounds have been documented in ancient Indian literature [37]. Over the last half century, known pharmacological effects of curcumin have been expanded to encompass antioxidant [38] and anti-inflammatory properties [39] as well as inhibition of tumorigenesis [40–42] and metastasis [43]. Despite its great potential for the treatment of diseases, curcumin's poor aqueous solubility, degradation and low bioavailability constitute major obstacles toward its medical deployment [44]. Heat treatment of curcumin [43] and the discovery of natural water soluble curcumin analogs [44, 45] have been suggested to overcome the stability and solubility issues in aqueous environments. Another approach to improve clinical applicability of curcumin has been to develop delivery vehicles that successfully transport the hydrophobic drug to *in vivo* target sites. Several formulations have been suggested for curcumin delivery. These include vehicles such as PLGA nanoparticles

[46], micellar polymer aggregates [47], polyvinyl alcohol hydrogels [48], and pluronic block copolymer micelles [36] as well as curcumin-casein micelles [49].

In this paper, we report the preparation and characterization of a curcumin-encapsulated, injectable, self-assembling peptide hydrogel system where curcumin encapsulation and peptide gelation is achieved concurrently in aqueous, physiological conditions. The ability of the solid gel material to immediately reform into a solid gel after shear-thinning/flow was studied with oscillatory rheology. In addition, *in vitro* cytotoxicity, the ability of released curcumin to induce programmed cell death (apoptosis) in medulloblastoma cancer cells was investigated. The characterization of the curcumin-impregnated hydrogel from the nanoscale through the macroscale reveals the great potential of this system as an injectable therapy system. The curcumin-loaded peptide hydrogel combines the features of minimally invasive delivery with the advantages of stabilizing curcumin and controlling its release. The rate of curcumin release and its consequent therapeutic efficacy can be conveniently controlled by changing the concentration of the MAX8 peptide.

2. Materials and Methods

2.1 Peptide Synthesis

MAX8 (95% purity) was produced and purified by New England Peptide (Gardner, MA, USA) according to previously published protocols [19,50].

2.2 Preparation of MAX8 Hydrogels

For the preparation of 0.5 wt% MAX8 hydrogel (0.5 mg MAX8 in 100 μl of hydrogel), 0.5 mg of MAX8 peptide is first dissolved in DI water. Self-assembly of the peptide is initiated with the addition of an equal volume of salt solution buffered to pH 7.4 or cell growth medium (pH 7.4). Buffer solutions used to trigger the self-assembly varied according to the nature of measurements. Buffers used were either cell culture media without fetal bovine serum (FBS) (ionic strength ~161 mM) or 100 mM BTP buffer (300 mM NaCl). The same protocol was used to prepare 1wt% and 2 wt% gels.

2.3 Preparation of Curcumin Loaded Hydrogels

Curcumin stock solutions in dimethyl sulfoxide (DMSO) were prepared 50× more concentrated than the final desired curcumin concentrations in hydrogels. The amount of curcumin stock solutions (DMSO) in hydrogels was fixed to 2% (v:v) for all DMSO-containing hydrogels. For example for 4 and 2 mM of curcumin-loaded hydrogels, 200 mM and 100 mM curcumin stock solutions were prepared in DMSO. Before the peptide hydrogel encapsulation process, curcumin stock solutions were added to DMEM cell-culture media to yield 4% (v:v) curcumin-DMSO:cell culture media. For example, 2 μl of 200 mM curcumin-DMSO stock was added to 48 μl of aqueous cell culture media. 50 μl of this curcumin in DMSO:cell culture media mixture was added to an appropriate peptide solution (0.5 mg MAX8 in 50 μl DI water) to yield 100 μl of 0.5 wt% MAX8 hydrogel loaded with 4mM curcumin. Likewise, 2 μl of 100 mM curcumin stock was diluted in 48 μl of cell culture media and added to the appropriate peptide solution to yield 100 μl of a 2 mM curcumin-loaded hydrogel. 0 mM curcumin samples were prepared by using DMSO without curcumin as stock solution. BTP buffer mix refers to solutions with (48:2:50) (v:v:v) BTP:DMSO stock:water. Cell culture mix refers to solutions with (48:2:50) (v:v:v) DMEM:DMSO stock:water.

2.4 Transmission Electron Microscopy

5 μl 0.5 wt% MAX8 hydrogel was applied to a carbon-coated grid and excess water was blotted away with filter paper. Fibrils were stained with uranyl acetate (1mg/ml). The grid

was left to dry in ambient conditions for ~ 2 hours. TEM was performed with JEOL JEM-2010f TEM operating at 200kV.

2.5 Fluorescence Studies

The interaction of curcumin with peptide was observed by fluorescence spectrophotometry. Fluorescence measurements were carried out in a Spex FluoroMax-7 spectrofluorometer (Horiba Jobin Yvon). Emission spectra were recorded from 450 to 700 nm with an excitation wavelength of 420 nm. For fluorescence measurements, peptide self-assembly was initiated in BTP buffer (pH 7.4) and 300mM NaCl to minimize the background scattering coming from cell-culture media. Final curcumin concentrations for this experiment were 0, 5, 10, 15 and 20 μM in 0.5 wt% hydrogel. 20 μM curcumin solutions in BTP buffer mix without peptide were used to determine spectroscopic characteristic of curcumin. Spectra were corrected by subtraction of the corresponding buffer signal.

2.6 Circular Dichroism

Circular dichroism (CD) spectra were collected on a Jasco (Tokyo, Japan) J-810 spectopolarimeter equipped with a Jasco PTC-424S Peltier temperature controller with a 1 mm quartz cell. The concentration of MAX8 was fixed at 0.15 mM. Curcumin stock solutions were prepared in ethanol and used as described previously. Samples were prepared using DMEM. Data collection was initiated after 60 minutes of sample preparation. Data is reported from 250 to 200 nm using a 2-nm step size at 37°C. Mean residue elipticity $[\theta] = (\theta_{obs}/10\times l\times c)/r$, where θ_{obs} is the measured elipticity in millidegrees, l is the length of the cell (in cm), c is the concentration (in M) and r is the number of residues. Spectra were corrected by subtraction of the corresponding buffer.

2.7 Oscillatory Rheology

Rheology experiments were conducted on TA instruments AR2000 stress-controlled rheometer with 20 mm-diameter acrylic, cross-hatched parallel plate geometry at 37°C. Samples were prepared as described previously with DMEM without phenol red. After mixing the peptide solution with the buffer solution to trigger intramolecular folding and consequent self-assembly into a hydrogel, the samples were loaded immediately onto the rheometer after which data collection was initiated. Dynamic time sweep experiments (DTS) were performed to monitor the storage (G′) and loss (G″) modulus as a function of time (6 rad/s frequency, 0.2% strain) for 60 minutes. For shear-thinning experiments, the samples were subjected to 1000 sec^{-1} shear for 30 seconds after which the strain was reduced to 0.2 %. Subsequently, recovery of the storage (G′) and loss (G″) modulus as a function of time (6 rad/s frequency, 0.2% strain) was monitored for 30 minutes. Dynamic frequency (0.1–100 rad/s frequency, 0.2% strain) sweep experiments were performed to establish the frequency response of the samples (Figure S2, Supporting information). Dynamic strain (0.1–1000% strain, 6 rad/s frequency) experiments were performed on samples to establish the linear viscoelastic region (Figure S3, Supporting information). All measurements were made in triplicate.

2.8 Cell culture

The human medulloblastoma cell line, DAOY cells, was obtained from American Type Culture Collection and cultured in DMEM supplemented with 10% fetal bovine serum, glutamine and penicillin/streptomycin (complete cell growth medium) in a humidified, 5% CO_2 atmosphere at 37°C.

2.9 Curcumin Hydrogels in Contact with DAOY cells

Curcumin hydrogels prepared with DMEM without FBS and phenol red (75 μL, 0.5 wt% MAX8 with 0 mM or 4 mM curcumin) were injected into a 35 mm cell culture dish. The samples were incubated overnight with 2 ml of phosphate buffered saline (PBS) solution at 37 °C and 95% humidity. The next day scaffolds were washed with PBS and cells were seeded at (10×10^4 cells/well (cm^2)) in complete cell growth medium covering the hydrogel and the tissue culture plastic (day 0). Optical micrographs were taken on day 1.

2.10 Curcumin Release Studies from Hydrogels

DAOY cells were plated in a 24-well plate (10×10^4 cells/well (cm^2)) and incubated overnight in complete cell culture medium. In a separate 24-well plate, MAX8 hydrogels encapsulating either 2 mM, 4 mM curcumin or DMSO alone were prepared as described previously in DMEM without phenol red. 75 μL of these samples were pipetted into corning transwell polyester membrane inserts (pore size 0.4 μM). The transwells were inserted into 24 well plates and incubated at 37°C for 3 hours in 2 ml PBS. After this step the PBS was replaced with fresh PBS to wash away any unencapsulated curcumin and the transwells were transferred into 24-well plates with DAOY cells. Light microscope images were taken on day 1. Images were slightly contrast-enhanced to improve visibility of the cell outline.

To determine curcumin release from hydrogels, 0.5wt%, 1 wt% and 2 wt% peptide hydrogels loaded with 4mM curcumin were prepared in triplicate with DMEM without phenol red as described previously, and 75 μL of the curcumin hydrogels were pipetted into corning 24-well transwell polyester membrane inserts. The transwells were inserted into 24 well plates and incubated at 37°C for 3 hours in 2 ml PBS. After this step the PBS was replaced with fresh PBS to wash away any unencapsulated curcumin. PBS was chosen to minimize background scattering. At each time point 100 μL of the respective well PBS supernatants were taken out and read in a black opaque 96-well microplate on a microplate reader (Perkin Elmer Victor™, USA). Emission at 535 nm was recorded with an excitation wavelength of 485 nm. The aliquots were returned to the wells after measurements. Released curcumin concentrations were estimated using a curcumin standard curve (Figure S6, Supporting Information). The slope of the PBS subtracted standard curve was used to correlate fluorescence intensities of supernatants to curcumin concentrations (Figure S6, Supporting Information).

2.11 *In Vitro* Cell Toxicity

LDH (lactate dehydrogenase) levels were determined using the non-radioactive cytotoxicity kit (Promega, Madison, WI) according to manufacturer's instructions. Samples were prepared as described previously and transferred into 0.4 μm pore size transwells. DAOY cells were plated in a 24-well plate (10×10^4 cells/well) and incubated with MAX8 hydrogels encapsulating either curcumin or DMSO alone. Released LDH was obtained from the media after centrifugation to remove cell debris. LDH from viable cells was collected by lysing the cells by freeze-thawing. Relative release of LDH was determined by the ratio of medium-released LDH versus total LDH (the sum of LDH in medium and viable cells). Assays were performed twice in triplicate.

2.12 Immunoblotting for Cell Apoptotic Markers

Cell lysates were prepared in a 1× SDS-lysis buffer (2% SDS) followed by sonication and centrifugation. Protein concentrations of the lysates were determined by Dc Protein assay (Bio-Rad, Hercules, CA). Equal amounts of protein were resolved by SDS-PAGE and then transferred to nitrocellulose membranes. Membranes were blocked using 5 % non-fat milk in tris-buffered saline with 0.1 % Tween 20 (TBS-T) and then incubated overnight at 4 °C

with primary antibodies diluted in 5 % bovine serum albumin/TBS-T. After incubation with HRP-conjugated secondary antibodies in 5 % non-fat milk/TBS-T, proteins of interest were visualized by Enhanced Chemiluminescence Plus (GE Healthcare, Piscataway, NJ).

3. Results and Discussion

3.1 Curcumin Interaction with MAX8 Peptide Hydrogel

The curcumin-hydrogel is prepared *in-situ* where curcumin encapsulation within the hydrogel network is accomplished concurrently with peptide self-assembly. The solubility of curcumin in aqueous solutions is limited but is enhanced in organic solvents such as dimethyl sulfoxide (DMSO), ethanol, methanol or acetone. We used DMSO, a non-toxic aprotic polar solvent, to help solubilize curcumin in aqueous solutions [51].

Curcumin, due to its polyphenolic structure, is a naturally fluorescent molecule [47]. The spectroscopic properties depend strongly on the nature of the local curcumin environment. To study the photophysical properties of curcumin in the presence of MAX8 peptide, we used fluorescence spectroscopy. Figure 2 overlays fluorescence bands of 0.5wt% MAX8 hydrogels at pH 7.4 assembled in bis-tris-propane (BTP) buffer with 0, 5, 10, 15 and 20 μM of curcumin. Figure 2 also displays the fluorescence spectrum of 20 μM curcumin in BTP buffer mixtures without peptide. Curcumin exhibits a broad and relatively weak fluorescence band maximum (Lmax) at ~ 550 nm in aqueous media without peptide. When MAX8 peptide is introduced into the system the signal is found to increase significantly and shift to a shorter wavelength regime (Lmax ~500 nm, blue shift). Our observations with fluorescence spectroscopy clearly indicate changes in curcumin microenvironment upon encapsulation within MAX8 hydrogel. Previous studies on interaction of curcumin with proteins have attributed an increase and blue shift in fluorescence signal to curcumin binding to hydrophobic regions of protein molecules [52,53]. Extending this argument to our system suggests significant curcumin interaction with hydrophobic peptide moieties. The phenolic hydrogens of curcumin have pKa values of 8.38, 9.88 and 10.51 in aqueous solutions [49,54]. At physiological pH (~7.4), curcumin is found in neutral form, hence binding due to charge interactions can be ignored [52]. Changes in microenvironment could arise from an interaction of the curcumin molecule with valine-rich faces in the core of assembled fibrils. When the amphiphilic MAX8 folds into a β-hairpin and subsequently self-assembles into fibrils, a hydrophobic layer is formed in the core of the fibrils. The valine side of the facially amphiphilic β-hairpins collapse to minimize interaction of hydrophobic domains with water. Our observations suggest that this hydrophobic core could participate in housing the hydrophobic curcumin molecules. Other possibilities of local hydrophobic environment for curcumin in the self-assembled gel include the hydrocarbon side chains of lysines or prolines exposed on the fibril surface. Finally, pure curcumin domains could be encapsulated by folded hairpin peptides and trapped within the assembled network.

3.2 β-Sheet and nanofibrillar hydrogel formation

The secondary structure of the MAX8 peptide in the absence and presence of curcumin was observed with circular dichroism (CD) spectroscopy (Figure 3). Data were recorded at 0.15 mM MAX8 with 0 mM, 0.08 mM or 0.4 mM curcumin. CD measurements require diluted, optically transparent systems. Curcumin-loaded hydrogels at high curcumin concentrations (e.g. 4 mM curcumin within 0.5 wt% MAX8 (1.5 mM peptide)) have high optical densities that interfere with CD measurement. Therefore, 0.15 mM MAX8 peptide solution was folded and assembled in the presence of 0.4 mM curcumin in order to lower the optical density of the samples as well as to keep the curcumin:peptide concentration ratio identical as the hydrogels studied for curcumin release. Data collection for samples was initiated after 60 minutes. The CD spectra of MAX8 peptide, with and without curcumin, exhibit minima

at 216 nm, indicative of β-sheet formation. The identical nature of the CD profiles clearly indicates that the presence of curcumin molecules during self-assembly of MAX8 peptide does not hinder β-hairpin folding and β-sheet formation.

TEM was used to investigate whether the fibrillar nanostructure formed by β-hairpin intermolecular assembly was affected by the presence of curcumin. Curcumin-containing hydrogels have the same characteristic appearance as neat peptide hydrogels with no discernable changes in fibril diameter or structure (Figure S1, Supporting Information). The data shows that the presence of curcumin, does not affect folding and subsequent self-assembly of the 20 amino acid MAX8 peptide into fibrils.

3.3 Oscillatory Rheology

Oscillatory rheology measurements were performed to observe gelation kinetics of 0.5 wt% MAX8 hydrogels (Figure 4(a)) and 0.5 wt% MAX8 hydrogels with 4mM curcumin (Figure 4(b)) before and after shear-thinning treatment. Gelation of freshly prepared samples was monitored for 60 minutes at a frequency of 6 rad s^{-1} and 0.2 % strain. Subsequently, steady shear (1000 s^{-1} for 30 seconds) was applied to the samples to mimic shear forces that would be exerted on samples during a syringe injection. Upon cessation of shear, recovery of network mechanical properties was monitored at 6 rad s^{-1} and 0.2% strain for 30 minutes. Dynamic frequency (0.1–100 rad s^{-1} frequency, 0.2% strain) sweep experiments were performed to establish the frequency response of the samples (Figure S2, Supporting Information). Dynamic strain (0.1–1000% strain, 6 rad s^{-1} frequency) experiments were performed on samples to establish the linear viscoelastic region (Figure S3, Supporting Information). Measurements were made in triplicate and average storage (G′) and loss (G″) modulus values (black data points) are shown in Figure 4. The average G′ and G″ for neat peptide hydrogels were measured as 315.0 ± 13.1 Pa and 11.0 ± 0.7 Pa after 60 minutes of initial assembly. The observed moduli directly after the shear-thinning treatment were 50.8 ± 17.1 and 12.2 ± 2.9 Pa, respectively, and 298.0 ± 28.0 Pa and 12.1 ± 0.7 Pa 30 minutes after the shear-thinning treatment. The values observed for hydrogels loaded with 4mM curcumin were 387.2 ± 39.0 Pa and 14.0 ± 1.0 Pa (at 60 minutes), 37.8 ± 8.8 Pa and 13.3 ± 1.7 Pa directly after shear-thinning and 330.1 ± 46.4 Pa and 13.0 ± 1.5 Pa 30 minutes after shear-thinning. Dynamic time (Figure S4, Supporting Information) and frequency sweep data (Figure S5, Supporting Information) for 0.5 wt% MAX 8 hydrogels with 2%v DMSO showing essentially no effect of the DMSO on peptide gelation, shear-thinning, and rehealing can be found in the supporting information.

We have recently reported structural and rheological analysis of hydrogel behavior during and after shear flow [55]. The proposed mechanism for the recovery after shear thinning involves gel network fracture into large (>200 nm) hydrogel domains under shear force that allows the gel to flow. The hydrogel domains immediately percolate upon cessation of shear force thus immediately producing a solid hydrogel. The boundaries between these immediately percolated domains further relax with time causing further stiffening of the gel close to pre-shear modulus values. The oscillatory rheology data here reveal that β-hairpin peptide hydrogel samples, both with or without curcumin, immediately display solid-like properties after shear thinning and quickly heal to stiffnesses close to pre-shear values. One difference between the neat hydrogels and the curcumin-loaded hydrogels is that the 4 mM curcumin loaded hydrogels are observed to be stiffer overall when compared to neat hydrogels. Curcumin has a strongly hydrophobic aliphatic bridge that separates the polar enolic and phenolic groups at the end and middle of the molecule [56]. Even though the polar groups diminish the hydrophobic character of the molecule, curcumin behaves like a hydrophobic molecule due to the highly hydrophobic bridge. Increased stiffening in curcumin hydrogels could be explained in several ways. It seems plausible that curcumin could be residing in the hydrophobic core of the fibrils, thus reducing relaxations of

hydrogen bonded fibrils making individual fibers stiffer yielding a stiffer network. Also, curcumin domains could be bridging different fibrils thus producing additional crosslinks in the network. Protein crosslinking by aromatic compounds as well as curcumin crosslinking of cystic fibrosis conductance channel (CFTR) peptides have been reported in literature [57]. Associations of each β-ketone in the symmetric curcumin molecule with the CFTR peptide as well as possible interaction with NH_2 moieties have been suggested. Accordingly, increased stiffening of curcumin-β-hairpin fibril hydrogels could also arise from cumulative effects of such mechanisms.

3.4 Curcumin Delivery and Cell Behavior

Figure 5a displays the bulk appearance of the 0.5 wt% hydrogel with 4 mM curcumin. Figure 5a and 5b compare self-supporting properties of 0.5 wt% MAX8 hydrogel with 4 mM curcumin and 4 mM curcumin in a BTP buffer:water mixture (1:1,v:v) without peptide, respectively. The pH of the curcumin loaded hydrogel was measured as 6.9. Digital images of inverted vials were taken after ~ 2 minutes of sample preparation. The color of the hydrogel in Figure 5a was significantly different from the color of the curcumin solution without peptide in Figure 5b. The color of the hydrogel loaded with 4 mM curcumin was red-orange whereas the BTP buffer mixture with 4 mM curcumin was orange-yellow. Similar optical behavior was observed in a study where curcumin was bound to β-amyloid fibrils [58].

The self-supporting nature of the hydrogels with or without curcumin generates a surface that allows us to monitor in vitro propagation of cells when cultured on the gels. It has been reported previously that curcumin induces cell death in various cancer cells, including the human medulloblastoma cell line DAOY (our unpublished data) [59,60]. While DAOY cells readily grew on hydrogel with no curcumin, curcumin-loaded gels inhibited their growth. Figure 5c and 5d display DAOY cells cultured on 0.5 wt% MAX8 loaded with 0 mM and 4 mM curcumin, respectively. After 24 hours, instances of attached DAOY cells could not be located on gels with curcumin (Figure 5d). Cells cultured on, and in the proximity of, the curcumin-loaded hydrogel displayed morphological features of cell death (cell rounding, shrinkage of cytoplasm, and detachment from tissue culture plate) whereas DAOY cells cultured on hydrogels lacking curcumin displayed attached and spread morphologies with no signs of visible cytotoxic effects caused by the MAX8 hydrogel itself (Figure 5c). Cell death observed both on and around, the curcumin-loaded hydrogel in Figure 5d clearly indicates the release of the curcumin from the peptide network.

To further investigate the bioactivity of released curcumin from the hydrogel, DAOY cells were seeded in 24 well plates and peptide hydrogels encapsulating different concentrations of curcumin were suspended in transwells with cell culture medium. After 24 hrs, DAOY cells showed morphological features of cell death when incubated with curcumin-encapsulated hydrogels (Figure 6a), while there were no evident signs of cell death in cells cultured with hydrogels without curcumin. Comparison of cells exposed to a fixed concentration of curcumin at a decreasing peptide concentration i.e. 2wt%, 1wt% and 0.5 wt % MAX8 hydrogels, showed signs of increased cell death. Also, the number of attached and well-spread DAOY cells were directly proportional to the peptide concentration (2wt%, 1wt % and 0.5 wt% MAX8 hydrogels) at a fixed mM curcumin. This could be explained by curcumin induced cell-cycle arrest and apoptosis observed in a variety of cancer cell lines *in vitro* [61–65]. This suggests that the peptide inhibits curcumin molecules from freely moving throughout the porous hydrogel network, primarily due to hydrophobic interactions (vide infra), thus causing slower drug release in hydrogels with higher peptide concentration. Together these results suggest that curcumin released from the hydrogel is biologically functional and that the release profile could be modulated as a function of the concentration of the MAX8 gel.

To test this possibility, MAX8 hydrogels at 0.5wt%, 1wt% and 2wt% of peptide, all at fixed curcumin concentration (4 mM), were prepared to quantify released curcumin into PBS supernatants (Figure 6(b)). Fluorescence intensities of supernatants were highest with 0.5 wt % β-hairpin peptide hydrogel, followed by 1wt% and 2 wt% hydrogels in descending order. This release profile was observed throughout the course of the measurement period. The amount of curcumin observed in all of the supernatants was found to be relatively stable over 3 days after which a slight decrease in the curcumin concentration was observed. Estimated curcumin concentrations in hydrogel supernatants over a two week period, as determined from a calibration curve (Figure S6, Supporting Information) of curcumin fluorescence in solution, varied from ~2.25 μM-3.25 μM for 2 wt% MAX8, ~2.75–3.75 μM for 1 wt% MAX8 and ~3.75–4.50 μM for 0.5 wt% MAX8 hydrogels encapsulating 4 mM curcumin. Therefore, even though the curcumin is constantly degrading in the supernatant as it is being released, the fluorescence is monitoring the active curcumin present in the supernatant that is available to effect cells. The curcumin release profiles are in agreement with the trend observed in Figure 6(a), where higher number of dead cells was observed in wells with lower peptide concentrations when loaded with the same curcumin concentration. Importantly, primary possible degradation products of curcumin: vanillin, ferulic acid and feruloyl methane, were measured to have negligible fluorescence at the settings used to measure fluorescence intensities of supernatants (Figure S7, Supporting Information).

The diffusion rates of solutes in physically crosslinked, semiflexible networks can be controlled by mesh size and specific or non-specific interactions between the macromolecules and the substrate [32,66]. The effect of the mesh size on the diffusion of a macromolecule through the network becomes prominent as the size of the molecule approaches the size of the network mesh.(32) In a previous study, the mesh size of the MAX8 fibril network was controlled by peptide weight percent. The mesh sizes of 0.5wt%, 1 wt% and 2 wt% MAX8 hydrogels formed under identical conditions were reported as 30±0.9, 23±0.4 and 18±0.3 nm respectively [32]. Therefore, the effect of mesh size on the mobility of the much smaller curcumin molecule should be negligible. Since curcumin is found in neutral form at physiological pH, binding due to charge interactions can be ignored. Therefore, the interaction of curcumin with hydrophobic functionalities on MAX8 peptide is believed to be an essential factor in the diffusion rate of curcumin. In the case of 2 wt% hydrogel, the amount of the hydrophobic functionalities possibly interacting with curcumin is increased relative to gels with lower peptide concentration, thus causing slower release of curcumin. Although the chemical stability of curcumin in blood or complete cell culture media (with 10% FBS) is superior to PBS, it still remains a major obstacle as almost 50% of the molecule is degraded within 8 hours [45]. Therefore, MAX8 peptide hydrogels create a reservoir from which curcumin is released slowly over a prolonged time period. Injection of the curcumin encapsulated hydrogel to a site *in vivo* could facilitate sustained release of the curcumin to surrounding tissues and/or blood stream.

To quantify cell death by hydrogel-released curcumin, released lactate dehydrogenase (LDH) levels were measured (Figure 6(c)). LDH is an enzyme that is released into the cell culture medium upon damage to the cell plasma membrane. Different concentrations of curcumin were encapsulated in 0.5 % hydrogel and then incubated with DAOY cells for 24 hrs. As shown in Figure 6(c), curcumin released from a hydrogel prepared with 4 mM of curcumin induced a higher amount of cytotoxicity compared to a hydrogel prepared with 2 mM curcumin which is in line with the cell death observed by phase contrast microscopy (Figure 6a). Contribution of possible curcumin degradation products (ferulic acid, feruloyl methane and vanillin) to the cytotoxicity of DAOY cells in this setting was found to be insignificant (Figure S8, Supporting Information).

Recently, IC50 values of curcumin towards DAOY cells have been reported as 25–50 μM in a study where the cells were treated with curcumin directly dispersed in cell culture media [67]. However, the IC50 concentrations are reported in the absence of a controlled release system. Biologically active curcumin concentrations in such systems over periods of days are difficult to quantify as reported half-life times for curcumin is ~ 8 hours [45]. Our data suggests that sustained release of curcumin, from the hydrogels, where the medium is continuously exposed to low concentrations of fresh curcumin, eliminates the need for high concentrations of curcumin to render DAOY cells susceptible to apoptosis.

The ability of curcumin to induce apoptosis in cancer cells through activation of caspase 3 and PARP has previously been reported [68]. Hydrogel-released curcumin induced cell death through apoptosis was tested by immunoblotting for caspase 3 and PARP. DAOY cells were exposed to 0, 2 and 4 mM curcumin-encapsulated 0.5, 1 and 2wt % hydrogels for 24 hrs. We found a dose-dependent increase of caspase 3 and PARP cleavage (Figure 7) that implies that the curcumin released from hydrogel is inducing apoptosis by similar mechanisms as non-encapsulated curcumin. In accordance with our results, cells exposed to hydrogel with a larger amount of peptide but with the same concentration of curcumin showed delayed apoptosis probably due to the lower amount of curcumin released from gels with higher peptide concentrations, as also observed with fluorescence and optical microscopy.

4. Conclusion

The results demonstrate a minimally invasive curcumin delivery strategy that can encapsulate and deliver sustained concentrations of curcumin locally to a delivery site. Oscillatory rheology measurements have revealed that β-hairpin peptide hydrogels with encapsulated curcumin concentrations as high as 4 mM immediately display solid-like properties after shear-thinning and reheal quickly over time to stiffnesses close to pre-shear values. Also, hydrogels loaded with 4 mM curcumin were found to be stiffer than hydrogels without curcumin. This could be due to curcumin residing in the hydrophobic core of the fibrils causing fibril stiffening or curcumin bridging different fibrils thus producing additional crosslinks in the network. Other possibilities of local hydrophobic environment for curcumin in the self-assembled gel include the hydrocarbon side chains of lysines or prolines exposed on the fibril surface. Finally, curcumin could be trapped within the assembled fibril network. It seems unlikely that curcumin encapsulation within the hydrogels is exclusive to one proposed mechanism, but, rather, a combination of mechanisms. *In vitro* experiments with a medulloblastoma cell line have shown that both curcumin released from hydrogel and directly applied to the cells induce caspase 3 mediated programmed cell death suggesting that curcumin encapsulation does not affect its biological activities. The combined physical and biological results clearly indicate the potential effectiveness of curcumin-loaded β-hairpin hydrogels as injectable agents for local curcumin delivery. *In vivo* studies with curcumin-hydrogel constructs to test their efficiencies in tumor models are currently underway.

Supplementary Material

Refer to Web version on PubMed Central for supplementary material.

Acknowledgments

AA and SJL have contributed equally to this work. This work was supported by the NIH COBRE P20 RR017716, American Cancer Society Research Grant RSG-09-021-01-CNE and funds from the Nemours Foundation to Sigrid A. Rajasekaran. We thank C. Ni, F. Kriss and the College of Engineering at the University of Delaware, for partial funding of W.M. Keck Electron Microscopy Facility.

References

[1]. Wichterle O, Lim D. Hydrophilic Gels for Biological Use. Nature. 1960; 185:117–8.

[2]. Van Tomme SR, Storm G, Hennink WE. In situ gelling hydrogels for pharmaceutical and biomedical applications. International Journal of Pharmaceutics. 2008; 355:1–18. [PubMed: 18343058]

[3]. Lee KY, Mooney DJ. Hydrogels for tissue engineering. Chemical Reviews. 2001; 101:1869–79. [PubMed: 11710233]

[4]. Hoffman AS. Hydrogels for biomedical applications. Advanced Drug Delivery Reviews. 2002; 54:3–12. [PubMed: 11755703]

[5]. Peppas NA, Hilt JZ, Khademhosseini A, Langer R. Hydrogels in biology and medicine: From molecular principles to bionanotechnology. Advanced Materials. 2006; 18:1345–60.

[6]. Vemula PK, Li J, John G. Enzyme catalysis: Tool to make and break amygdalin hydrogelators from renewable resources: A delivery model for hydrophobic drugs. Journal of the American Chemical Society. 2006; 128:8932–8. [PubMed: 16819889]

[7]. Slaughter BV, Khurshid SS, Fisher OZ, Khademhosseini A, Peppas NA. Hydrogels in Regenerative Medicine. Advanced Materials. 2009; 21:3307–29. [PubMed: 20882499]

[8]. Hatefi A, Amsden B. Biodegradable injectable in situ forming drug delivery systems. Journal of Controlled Release. 2002; 80:9–28. [PubMed: 11943384]

[9]. Chitkara D, Shikanov A, Kumar N, Domb AJ. Biodegradable injectable in situ depot-forming drug delivery systems. Macromolecular Bioscience. 2006; 6:977–90. [PubMed: 17128422]

[10]. Mosiewicz KA, Johnsson K, Lutolf MP. Phosphopantetheinyl Transferase-Catalyzed Formation of Bioactive Hydrogels for Tissue Engineering. Journal of the American Chemical Society. 2010; 132:5972–4. [PubMed: 20373804]

[11]. Beaty CE, Saltzman WM. Controlled Growth-Factor Delivery Induces Differential Neurite Outgrowth in 3-Dimensional Cell-Cultures. Journal of Controlled Release. 1993; 24:15–23.

[12]. Kim S, Healy KE. Synthesis and characterization of injectable poly(N-isopropylacrylamide-co-acrylic acid) hydrogels with proteolytically degradable cross-links. Biomacromolecules. 2003; 4:1214–23. [PubMed: 12959586]

[13]. Farokhzad OC, Langer R. Impact of Nanotechnology on Drug Delivery. Acs Nano. 2009; 3:16–20. [PubMed: 19206243]

[14]. Ozbas B, Kretsinger J, Rajagopal K, Schneider JP, Pochan DJ. Salt-triggered peptide folding and consequent self-assembly into hydrogels with tunable modulus. Macromolecules. 2004; 37:7331–7.

[15]. Pochan DJ, Schneider JP, Kretsinger J, Ozbas B, Rajagopal K, Haines L. Thermally reversible hydrogels via intramolecular folding and consequent self-assembly of a de Novo designed peptide. Journal of the American Chemical Society. 2003; 125:11802–3. [PubMed: 14505386]

[16]. Zhang SG. Fabrication of novel biomaterials through molecular self-assembly. Nature Biotechnology. 2003; 21:1171–8.

[17]. Wang C, Stewart RJ, Kopecek J. Hybrid hydrogels assembled from synthetic polymers and coiled-coil protein domains. Nature. 1999; 397:417–20. [PubMed: 9989405]

[18]. Petka WA, Harden JL, McGrath KP, Wirtz D, Tirrell DA. Reversible hydrogels from self-assembling artificial proteins. Science. 1998; 281:389–92. [PubMed: 9665877]

[19]. Schneider JP, Pochan DJ, Ozbas B, Rajagopal K, Pakstis L, Kretsinger J. Responsive hydrogels from the intramolecular folding and self-assembly of a designed peptide. Journal of the American Chemical Society. 2002; 124:15030–7. [PubMed: 12475347]

[20]. Paramonov SE, Jun HW, Hartgerink JD. Self-assembly of peptide-amphiphile nanofibers: The roles of hydrogen bonding and amphiphilic packing. Journal of the American Chemical Society. 2006; 128:7291–8. [PubMed: 16734483]

[21]. Aggeli A, Bell M, Boden N, Keen JN, Knowles PF, McLeish TCB, et al. Responsive gels formed by the spontaneous self-assembly of peptides into polymeric beta-sheet tapes. Nature. 1997; 386:259–62. [PubMed: 9069283]

[22]. Sutton S, Campbell NL, Cooper AI, Kirkland M, Frith WJ, Adams DJ. Controlled Release from Modified Amino Acid Hydrogels Governed by Molecular Size or Network Dynamics. Langmuir. 2009; 25:10285–91. [PubMed: 19499945]

[23]. Wheeldon IR, Barton SC, Banta S. Bioactive proteinaceous hydrogels from designed bifunctional building blocks. Biomacromolecules. 2007; 8:2990–4. [PubMed: 17887795]

[24]. Foo C, Lee JS, Mulyasasmita W, Parisi-Amon A, Heilshorn SC. Two-component protein-engineered physical hydrogels for cell encapsulation. Proceedings of the National Academy of Sciences of the United States of America. 2009; 106:22067–72. [PubMed: 20007785]

[25]. Ramachandran S, Tseng Y, Yu YB. Repeated rapid shear-responsiveness of peptide hydrogels with tunable shear modulus. Biomacromolecules. 2005; 6:1316–21. [PubMed: 15877347]

[26]. Banwell EF, Abelardo ES, Adams DJ, Birchall MA, Corrigan A, Donald AM, et al. Rational design and application of responsive alpha-helical peptide hydrogels. Nature Materials. 2009; 8:596–600.

[27]. Guilbaud JB, Vey E, Boothroyd S, Smith AM, Ulijn RV, Saiani A, et al. Enzymatic Catalyzed Synthesis and Triggered Gelation of Ionic Peptides. Langmuir. 2010; 26:11297–303. [PubMed: 20408518]

[28]. Chung HJ, Park TG. Self-assembled and nanostructured hydrogels for drug delivery and tissue engineering. Nano Today. 2009; 4:429–37.

[29]. Hule RA, Nagarkar RP, Altunbas A, Ramay HR, Branco MC, Schneider JP, et al. Correlations between structure, material properties and bioproperties in self-assembled beta-hairpin peptide hydrogels. Faraday Discussions. 2008; 139:251–64. [PubMed: 19048999]

[30]. Haines-Butterick L, Rajagopal K, Branco M, Salick D, Rughani R, Pilarz M, et al. Controlling hydrogelation kinetics by peptide design for three-dimensional encapsulation and injectable delivery of cells. Proceedings of the National Academy of Sciences of the United States of America. 2007; 104:7791–6. [PubMed: 17470802]

[31]. Nagarkar RP, Hule RA, Pochan DJ, Schneider JP. De novo design of strand-swapped beta-hairpin hydrogels. Journal of the American Chemical Society. 2008; 130:4466–74. [PubMed: 18335936]

[32]. Branco MC, Pochan DJ, Wagner NJ, Schneider JP. Macromolecular diffusion and release from self-assembled beta-hairpin peptide hydrogels. Biomaterials. 2009; 30:1339–47. [PubMed: 19100615]

[33]. Yan CQ, Pochan DJ. Rheological properties of peptide-based hydrogels for biomedical and other applications. Chemical Society Reviews. 2010; 39:3528–40. [PubMed: 20422104]

[34]. Rajagopal K, Ozbas B, Pochan DJ, Schneider JP. Probing the importance of lateral hydrophobic association in self-assembling peptide hydrogelators. European Biophysics Journal with Biophysics Letters. 2006; 35:162–9. [PubMed: 16283291]

[35]. Yucel T, Micklitsch CM, Schneider JP, Pochan DJ. Direct observation of early-time hydrogelation in beta-hairpin peptide self-assembly. Macromolecules. 2008; 41:5763–72. [PubMed: 19169385]

[36]. Sahu A, Kasoju N, Goswami P, Bora U. Encapsulation of Curcumin in Pluronic Block Copolymer Micelles for Drug Delivery Applications. Journal of Biomaterials Applications. 2010; 00:1–21.

[37]. Goel A, Kunnumakkara AB, Aggarwal BB. Curcumin as “Curecumin”: From kitchen to clinic. Biochemical Pharmacology. 2008; 75:787–809. [PubMed: 17900536]

[38]. Ruby AJ, Kuttan G, Babu KD, Rajasekharan KN, Kuttan R. Antitumor and Antioxidant Activity of Natural Curcuminoids. Cancer Letters. 1995; 94:79–83. [PubMed: 7621448]

[39]. Lantz RC, Chen GJ, Solyom AM, Jolad SD, Timmermann BN. The effect of turmeric extracts on inflammatory mediator production. Phytomedicine. 2005; 12:445–52. [PubMed: 16008121]

[40]. Aggarwal BB, Kumar A, Bharti AC. Anticancer potential of curcumin: Preclinical and clinical studies. Anticancer Research. 2003; 23:363–98. [PubMed: 12680238]

[41]. Shi MX, Cai QF, Yao LM, Mao YB, Ming YL, Ouyang GL. Antiproliferation and apoptosis induced by curcumin in human ovarian cancer cells. Cell Biology International. 2006; 30:221–6. [PubMed: 16376585]

[42]. Surh YJ. Anti-tumor promoting potential of selected spice ingredients with antioxidative and anti-inflammatory activities: a short review. Food and Chemical Toxicology. 2002; 40:1091–7. [PubMed: 12067569]

[43]. Kurien BT, Singh A, Matsumoto H, Scofield RH. Improving the solubility and pharmacological efficacy of curcumin by heat treatment. Assay and Drug Development Technologies. 2007; 5:567–76. [PubMed: 17767425]

[44]. Anand P, Thomas SG, Kunnumakkara AB, Sundaram C, Harikumar KB, Sung B, et al. Biological activities of curcumin and its analogues (Congeners) made by man and Mother Nature. Biochemical Pharmacology. 2008; 76:1590–1611. [PubMed: 18775680]

[45]. Basile V, Ferrari E, Lazzari S, Belluti S, Pignedoli F, Imbriano C. Curcumin derivatives: Molecular basis of their anti-cancer activity. Biochemical Pharmacology. 2009; 78:1305–15. [PubMed: 19580791]

46. Anand P, Nair HB, Sung BK, Kunnumakkara AB, Yadav VR, Tekmal RR, et al. Design of curcumin-loaded PLGA nanoparticles formulation with enhanced cellular uptake, and increased bioactivity in vitro and superior bioavailability in vivo. Biochemical Pharmacology. 2010; 79:330–8. [PubMed: 19735646]

[47]. Bisht S, Feldmann G, Soni S, Rajani R, Karikar C, Maitra A, et al. Polymeric nanoparticle-encapsulated curcumin (“nanocurcumin”):a novel strategy for human cancer therapy. Journal of Nanobiotechnology. 2007; 5:1–18. [PubMed: 17295922]

[48]. Shah CP, Mishra B, Kumar M, Priyadarsini KI, Bajaj PN. Binding studies of curcumin to polyvinyl alcohol/polyvinyl alcohol hydrogel and its delivery to liposomes. Current Science. 2008; 95:1426–32.

[49]. Sahu A, Bora U, Kasoju N, Goswami P. Synthesis of novel biodegradable and self-assembling methoxy poly(ethylene glycol)-palmitate nanocarrier for curcumin delivery to cancer cells. Acta Biomaterialia. 2008; 4:1752–61. [PubMed: 18524701]

[50]. Nagarkar, RP.; Schneider, JP. Synthesis and Primary Characterization of Self-Assembled Peptide-Based Hydrogels. In: Gazit, E.; Nussinov, R., editors. Nanostructure Design: Methods and Protocols. Humana Press; Totowa, NJ: 2008. p. 61-77.

[51]. Simth ER, Hadidian Z, Mason MM. Single-and Repeated-Dose Toxicity of Dimethyl Sulfoxide. Annals of the New York Academy of Sciences. 1967; 141:96–109. [PubMed: 4962802]

[52]. Sahu A, Kasoju N, Bora U. Fluorescence Study of the Curcumin-Casein Micelle Complexation and Its Application as a Drug Nanocarrier to Cancer Cells. Biomacromolecules. 2008; 9:2905–12. [PubMed: 18785706]

[53]. Yu HL, Huang QR. Enhanced in vitro anti-cancer activity of curcumin encapsulated in hydrophobically modified starch. Food Chemistry. 2010; 119:669–74.

[54]. Bernabe-Pineda M, Ramirez-Silva MT, Romero-Romo M, Gonzadlez-Vergara E, Rojas-Hernandez A. Determination of acidity constants of curcumin in aqueous solution and apparent rate constant of its decomposition. Spectrochimica Acta Part a-Molecular and Biomolecular Spectroscopy. 2004; 60:1091–7.

[55]. Yan CQ, Altunbas A, Yucel T, Nagarkar RP, Schneider JP, Pochan DJ. Injectable solid hydrogel: mechanism of shear-thinning and immediate recovery of injectable beta-hairpin peptide hydrogels. Soft Matter. 2010; 6:5143–56. [PubMed: 21566690]

[56]. Balasubramanian K. Molecular orbital basis for yellow curry spice curcumin's prevention of Alzheimer's disease. Journal of Agricultural and Food Chemistry. 2006; 54:3512–20. [PubMed: 19127718]

[57]. Bernard K, Wang W, Narlawar R, Schmidt B, Kirk KL. Curcumin Cross-links Cystic Fibrosis Transmembrane Conductance Regulator (CFTR) Polypeptides and Potentiates CFTR Channel Activity by Distinct Mechanisms. Journal of Biological Chemistry. 2009; 284:30754–65. [PubMed: 19740743]

[58]. Yanagisawa D, Shirai N, Amatsubo T, Taguchi H, Hirao K, Urushitani M, et al. Relationship between the tautomeric structures of curcumin derivatives and their A beta-binding activities in the context of therapies for Alzheimer's disease. Biomaterials. 2010; 31:4179–85. [PubMed: 20181392]

[59]. Syng-ai C, Kumari AL, Khar A. Effect of curcumin on normal and tumor cells: Role of glutathione and bcl-2. Molecular Cancer Therapeutics. 2004; 3:1101–8. [PubMed: 15367704]

[60]. Ravindran J, Prasad S, Aggarwal BB. Curcumin and Cancer Cells: How Many Ways Can Curry Kill Tumor Cells Selectively? Aaps Journal. 2009; 11:495–510. [PubMed: 19590964]

[61]. Sharma RA, Gescher AJ, Steward WP. Curcumin: The story so far. European Journal of Cancer. 2005; 41:1955–68. [PubMed: 16081279]

[62]. Duvoix A, Blasius R, Delhalle S, Schnekenburger M, Morceau F, Henry E, et al. Chemopreventive and therapeutic effects of curcumin. Cancer Letters. 2005; 223:181–90. [PubMed: 15896452]

[63]. Surh, YJ.; Chun, KS. Molecular Targets and Therapeutic Uses of Curcumin in Health and Disease. 2007. Cancer chemopreventive effects of curcumin; p. 149-72.

[64]. Kuttan, G.; Kumar, KBH.; Guruvayoorappan, C.; Kuttan, R. Molecular Targets and Therapeutic Uses of Curcumin in Health and Disease. 2007. Antitumor, anti-invasion, and antimetastatic effects of curcumin; p. 173-84.

[65]. Kunnumakkara AB, Anand P, Aggarwal BB. Curcumin inhibits proliferation, invasion, angiogenesis and metastasis of different cancers through interaction with multiple cell signaling proteins. Cancer Letters. 2008; 269:199–225. [PubMed: 18479807]

[66]. Branco MC, Pochan DJ, Wagner NJ, Schneider JP. The effect of protein structure on their controlled release from an injectable peptide hydrogel. Biomaterials. 2010; 31:9527–34. [PubMed: 20952055]

[67]. Bangaru MLY, Chen SL, Woodliff J, Kansra S. Curcumin (Diferuloylmethane) Induces Apoptosis and Blocks Migration of Human Medulloblastoma Cells. Anticancer Research. 2010; 30:499–504. [PubMed: 20332461]

[68]. Moragoda L, Jaszewski R, Majumdar APN. Curcumin induced modulation of cell cycle and apoptosis in gastric and colon cancer cells. Anticancer Research. 2001; 21:873–8. [PubMed: 11396178]

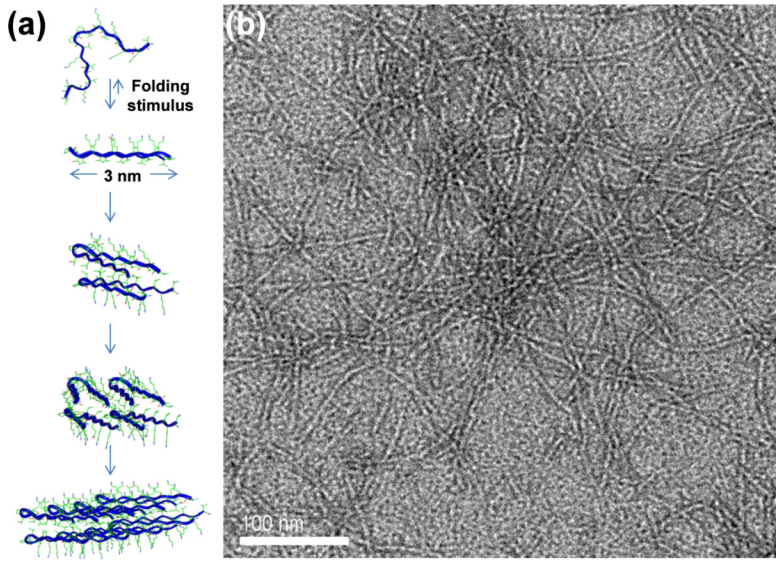

Fig. 1.
(a) Schematic for self-assembly of MAX8 peptide (b) Transmission electron microscopy image of negatively stained MAX8 fibrils.

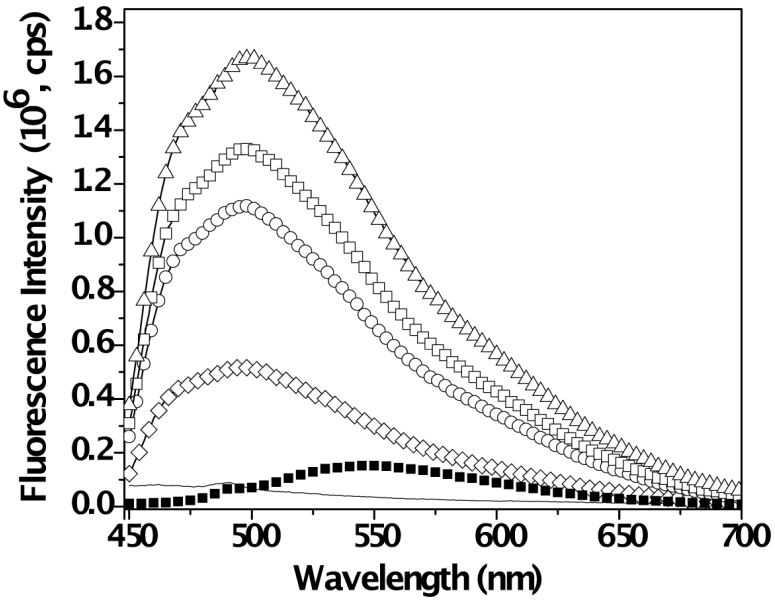

Fig. 2.

Overlay of fluorescence signals obtained from 0.5wt% MAX8 hydrogel with 0 (−), 5 (◊), 10 (◯), 15 (□) and 20 μM (△) curcumin and 20 μM of curcumin in BTP buffer at pH 7.4 without peptide (■).

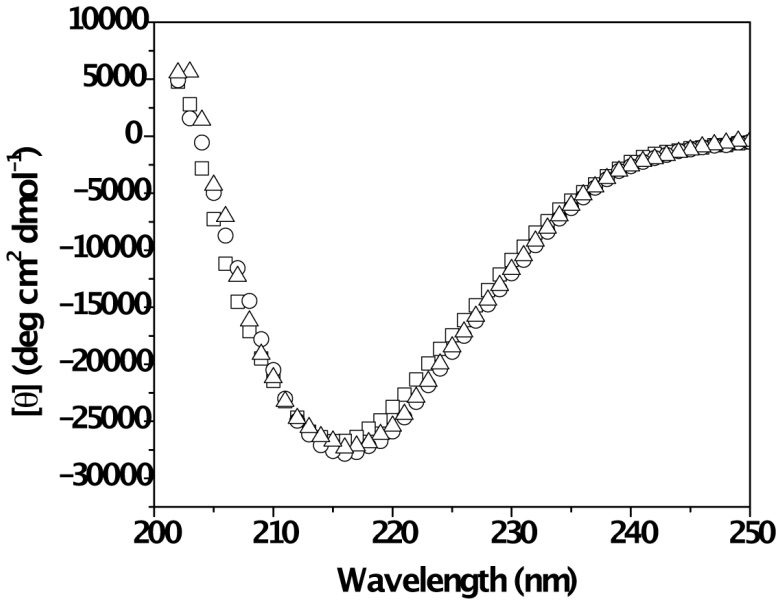

Fig. 3.

Circular Dichroism (CD) spectra of 0.15 mM MAX8 peptide in buffer solution (□), 0.15 mM MAX8 peptide in buffer solution with 0.08 mM curcumin (◯) and 0.15 mM MAX8 peptide in buffer solution with 0.4 mM curcumin.

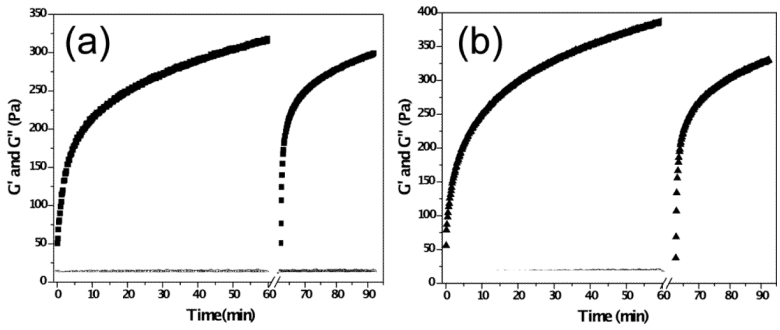

Fig. 4.

(a) Oscillatory rheology and shear-thin recovery of 0.5 wt% MAX8 hydrogel prepared in DMEM (■=G′ and ◯=G″) (b) Oscillatory rheology and shear-thin recovery of 0.5 wt% MAX8 hydrogel prepared with DMEM and 4 mM curcumin (▲= G′ and △=G″). Measurements are made in triplicate at 37°C. Data points represent average values.

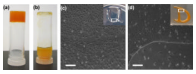

Fig. 5.

(a) 0.5 wt% MAX8 hydrogel with 4 mM curcumin in an upturned vial (reddish-orange) (b) 4 mM curcumin in BTP buffer mix without MAX8 peptide in an upturned vial (orangish-yellow) (c) DAOY cells seeded on 0.5wt% MAX8 hydrogels with 0 mM curcumin and tissue culture plastic (d) DAOY cells seeded on 0.5wt% MAX8 hydrogels with 2 mM curcumin and tissue culture plastic. The white boxes in Fig5c and Fig5d insets represent the area where the optical microscopy images were taken. Scale bars represent 200 μm.

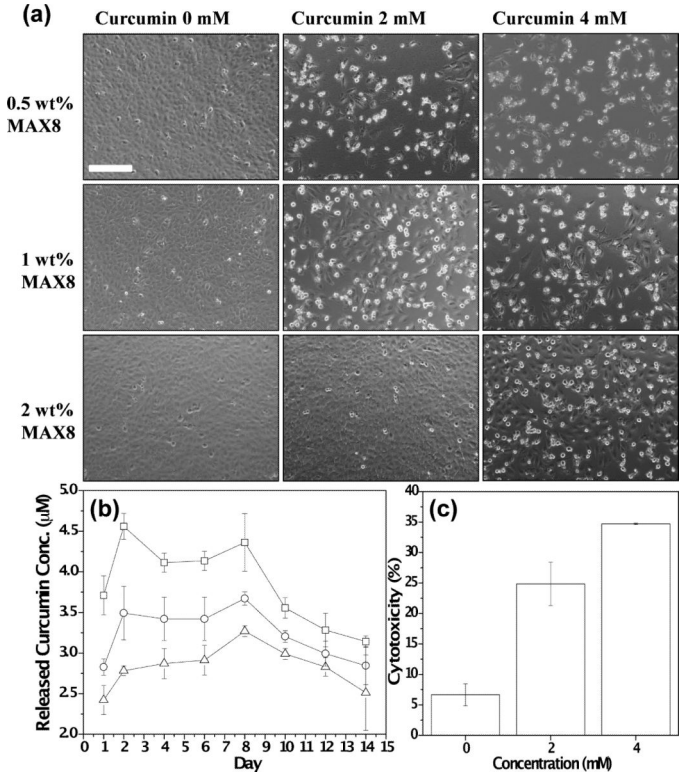

Fig. 6.

(a) Effect of released curcumin from 0.5 wt%, 1 wt% and 2 wt% MAX8 gels prepared with 0 mM, 2 mM and 4 mM curcumin on DAOY cells. Cell rounding and detachment as indicator of cell death where found only in the presence of curcumin-encapsulated hydrogels but not with curcumin-free control gels (b) Curcumin concentration released into PBS supernatants from 0.5wt% (□), 1wt% (◯) and 2wt% (△) MAX8 hydrogels prepared at fixed curcumin concentration (4 mM) (c) Cytotoxic effect of curcumin as determined by released lactate dehydrogenase (LDH) levels. 0.5 wt% MAX8 hydrogels prepared at 0 mM, 2 mM and 4 mM curcumin concentrations. Scale bar represents 200 μm.

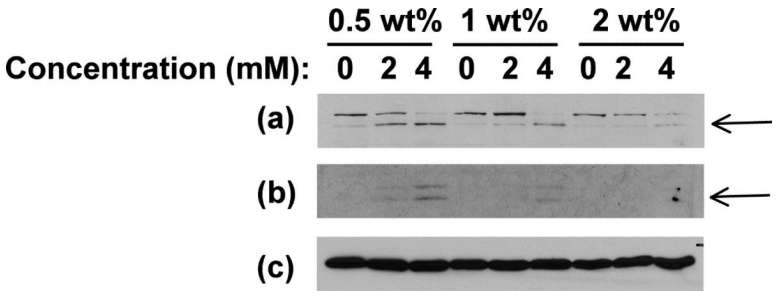

Fig. 7.

Immunoblot for apoptotic marker proteins, (a) cleaved PARP and (b) cleaved caspase 3, in DAOY cells exposed to curcumin released from 0.5wt%, 1 wt% and 2 wt% β-hairpin gels encapsulating 0, 2 and 4 mM initial curcumin concentration. (c) Immunoblot for β-tubulin confirms equal loading. Arrows indicate cleaved PARP and Caspase 3 respectively.